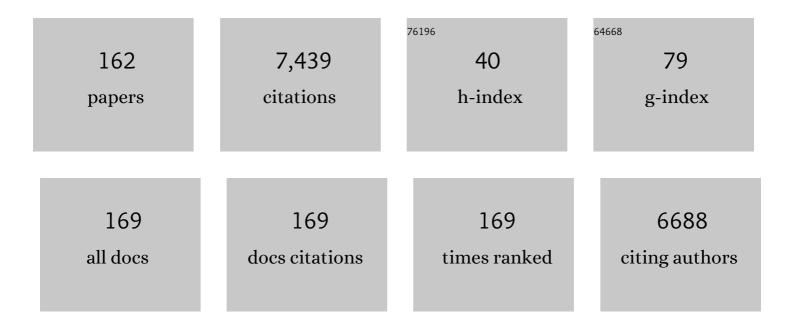
Xinwei Wang

List of Publications by Year in descending order

Source: https://exaly.com/author-pdf/6880405/publications.pdf

Version: 2024-02-01



#	Article	IF	CITATIONS
1	Thermal Conductivity of Nanoparticle - Fluid Mixture. Journal of Thermophysics and Heat Transfer, 1999, 13, 474-480.	0.9	2,002
2	Thermopower enhancement in conducting polymer nanocomposites via carrier energy scattering at the organic–inorganic semiconductor interface. Energy and Environmental Science, 2012, 5, 8351.	15.6	351
3	Temperature Dependence of Electrical and Thermal Conduction in Single Silver Nanowire. Scientific Reports, 2015, 5, 10718.	1.6	149
4	New Secrets of Spider Silk: Exceptionally High Thermal Conductivity and Its Abnormal Change under Stretching. Advanced Materials, 2012, 24, 1482-1486.	11.1	146
5	Thermal characterization of microscale conductive and nonconductive wires using transient electrothermal technique. Journal of Applied Physics, 2007, 101, 063537.	1.1	145
6	Generalized theory of the photoacoustic effect in a multilayer material. Journal of Applied Physics, 1999, 86, 3953-3958.	1.1	121
7	Interface-mediated extremely low thermal conductivity of graphene aerogel. Carbon, 2016, 98, 381-390.	5.4	120
8	Nanoscale thermal probing. Nano Reviews, 2012, 3, 11586.	3.7	119
9	Thermal diffusivity and conductivity of multiwalled carbon nanotube arrays. Physics Letters, Section A: General, Atomic and Solid State Physics, 2007, 369, 120-123.	0.9	116
10	Thermal Transport in Graphene Nanostructures: Experiments and Simulations. ECS Transactions, 2010, 28, 73-83.	0.3	110
11	Micro/Nanoscale Spatial Resolution Temperature Probing for the Interfacial Thermal Characterization of Epitaxial Graphene on 4Hâ€SiC. Small, 2011, 7, 3324-3333.	5.2	102
12	Thermal properties of carbon nanotube array used for integrated circuit cooling. Journal of Applied Physics, 2006, 100, 074302.	1.1	95
13	Photo-Acoustic Measurement of Thermal Conductivity of Thin Films and Bulk Materials. Journal of Heat Transfer, 2001, 123, 138-144.	1.2	88
14	Novel Polyethylene Fibers of Very High Thermal Conductivity Enabled by Amorphous Restructuring. ACS Omega, 2017, 2, 3931-3944.	1.6	83
15	Noncontact thermal characterization of multiwall carbon nanotubes. Journal of Applied Physics, 2005, 97, 064302.	1.1	81
16	Molecular Dynamics Simulation of Heat Transfer and Phase Change During Laser Material Interaction. Journal of Heat Transfer, 2002, 124, 265-274.	1.2	78
17	Rough contact is not always bad for interfacial energy coupling. Nanoscale, 2013, 5, 11598.	2.8	71
18	Interfacial thermal conductance between few to tens of layered-MoS2 and c-Si: Effect of MoS2 thickness. Acta Materialia, 2017, 122, 152-165.	3.8	67

#	Article	IF	CITATIONS
19	Dynamic response of graphene to thermal impulse. Physical Review B, 2011, 84, .	1.1	66
20	Significantly reduced thermal diffusivity of free-standing two-layer graphene in graphene foam. Nanotechnology, 2013, 24, 415706.	1.3	58
21	Raman-based Nanoscale Thermal Transport Characterization: A Critical Review. International Journal of Heat and Mass Transfer, 2020, 154, 119751.	2.5	55
22	Five Orders of Magnitude Reduction in Energy Coupling across Corrugated Graphene/Substrate Interfaces. ACS Applied Materials & Interfaces, 2014, 6, 2809-2818.	4.0	53
23	Molecular dynamics simulation of thermal and thermomechanical phenomena in picosecond laser material interaction. International Journal of Heat and Mass Transfer, 2003, 46, 45-53.	2.5	51
24	Measurement of the thermal conductivities of suspended MoS ₂ and MoSe ₂ by nanosecond ET-Raman without temperature calibration and laser absorption evaluation. Nanoscale, 2018, 10, 23087-23102.	2.8	51
25	The defect level and ideal thermal conductivity of graphene uncovered by residual thermal reffusivity at the 0 K limit. Nanoscale, 2015, 7, 10101-10110.	2.8	50
26	Thermal conductivity and annealing effect on structure of lignin-based microscale carbon fibers. Carbon, 2017, 121, 35-47.	5.4	50
27	Switch on the high thermal conductivity of graphene paper. Nanoscale, 2016, 8, 17581-17597.	2.8	49
28	Significant Radiation Tolerance and Moderate Reduction in Thermal Transport of a Tungsten Nanofilm by Inserting Monolayer Graphene. Advanced Materials, 2017, 29, 1604623.	11.1	49
29	Thermal characterization of single-wall carbon nanotube bundles using the self-heating 3ï‰ technique. Journal of Applied Physics, 2006, 100, 124314.	1.1	48
30	Thermal Conductivity of Ultrahigh Molecular Weight Polyethylene Crystal: Defect Effect Uncovered by 0 K Limit Phonon Diffusion. ACS Applied Materials & Interfaces, 2015, 7, 27279-27288.	4.0	48
31	Inkjet Printing of Singleâ€Crystalline Bi ₂ Te ₃ Thermoelectric Nanowire Networks. Advanced Electronic Materials, 2017, 3, 1600524.	2.6	48
32	Frequency-domain energy transport state-resolved Raman for measuring the thermal conductivity of suspended nm-thick MoSe2. International Journal of Heat and Mass Transfer, 2019, 133, 1074-1085.	2.5	48
33	Thermal Diffusivity of a Single Carbon Nanocoil: Uncovering the Correlation with Temperature and Domain Size. ACS Nano, 2016, 10, 9710-9719.	7.3	47
34	The hot carrier diffusion coefficient of sub-10 nm virgin MoS ₂ : uncovered by non-contact optical probing. Nanoscale, 2017, 9, 6808-6820.	2.8	46
35	Photothermal phenomenon: Extended ideas for thermophysical properties characterization. Journal of Applied Physics, 2022, 131, .	1.1	46
36	Nonmonotonic thickness-dependence of in-plane thermal conductivity of few-layered MoS ₂ : 2.4 to 37.8 nm. Physical Chemistry Chemical Physics, 2018, 20, 25752-25761.	1.3	45

#	Article	IF	CITATIONS
37	Thermal transport in multiwall carbon nanotube buckypapers. Physics Letters, Section A: General, Atomic and Solid State Physics, 2010, 374, 4144-4151.	0.9	44
38	Large-scale molecular dynamics simulation of surface nanostructuring with a laser-assisted scanning tunnelling microscope. Journal Physics D: Applied Physics, 2005, 38, 1805-1823.	1.3	42
39	Highly Efficient Method for Preparing Homogeneous and Stable Colloids Containing Graphene Oxide. Nanoscale Research Letters, 2011, 6, 47.	3.1	42
40	Graphene Aerogel Based Bolometer for Ultrasensitive Sensing from Ultraviolet to Far-Infrared. ACS Nano, 2019, 13, 5385-5396.	7.3	42
41	Noncontact Sub-10 nm Temperature Measurement in Near-Field Laser Heating. ACS Nano, 2011, 5, 4466-4475.	7.3	41
42	Thermal conductivity and secondary porosity of single anatase TiO ₂ nanowire. Nanotechnology, 2012, 23, 185701.	1.3	41
43	Thermal and Electrical Conduction in Ultrathin Metallic Films: 7 nm down to Subâ€Nanometer Thickness. Small, 2013, 9, 2585-2594.	5.2	41
44	Thermal transport in bent graphenenanoribbons. Nanoscale, 2013, 5, 734-743.	2.8	41
45	Promoted electron transport and sustained phonon transport by DNA down to 10ÂK. Polymer, 2014, 55, 6373-6380.	1.8	41
46	Energy Transport State Resolved Raman for Probing Interface Energy Transport and Hot Carrier Diffusion in Few-Layered MoS ₂ . ACS Photonics, 2017, 4, 3115-3129.	3.2	41
47	Effect of temperature on Raman intensity of nm-thick WS ₂ : combined effects of resonance Raman, optical properties, and interface optical interference. Nanoscale, 2020, 12, 6064-6078.	2.8	41
48	Transient thermal characterization of micro/submicroscale polyacrylonitrile wires. Applied Physics A: Materials Science and Processing, 2007, 89, 153-156.	1.1	40
49	Development of pulsed laser-assisted thermal relaxation technique for thermal characterization of microscale wires. Journal of Applied Physics, 2008, 103, .	1.1	40
50	Thermophysical properties of multi-wall carbon nanotube bundles at elevated temperatures up to 830K. Carbon, 2011, 49, 1680-1691.	5.4	40
51	Development of time-domain differential Raman for transient thermal probing of materials. Optics Express, 2015, 23, 10040.	1.7	40
52	Thermo-physical properties of thin films composed of anatase TiO2 nanofibers. Acta Materialia, 2011, 59, 1934-1944.	3.8	39
53	Potential of producing carbon fiber from biorefinery corn stover lignin with high ash content. Journal of Applied Polymer Science, 2018, 135, 45736.	1.3	39
54	Electron Transport and Bulk-like Behavior of Wiedemann–Franz Law for Sub-7 nm-Thin Iridium Films on Silkworm Silk. ACS Applied Materials & Interfaces, 2014, 6, 11341-11347.	4.0	37

#	Article	IF	CITATIONS
55	Frequency-resolved Raman for transient thermal probing and thermal diffusivity measurement. Optics Letters, 2016, 41, 80.	1.7	37
56	Anisotropic thermal conductivities and structure in lignin-based microscale carbon fibers. Carbon, 2019, 147, 58-69.	5.4	37
57	Thermal and electrical conduction in 6.4 nm thin gold films. Nanoscale, 2013, 5, 4652.	2.8	36
58	Thermoelectric properties of solution-synthesized n-type Bi2Te3 nanocomposites modulated by Se: An experimental and theoretical study. Nano Research, 2016, 9, 117-127.	5.8	36
59	Thermal characterization of carbon nanotube fiber by time-domain differential Raman. Carbon, 2016, 103, 101-108.	5.4	35
60	Thermal characterization of micro/nanoscale conductive and non-conductive wires based on optical heating and electrical thermal sensing. Journal Physics D: Applied Physics, 2006, 39, 3362-3370.	1.3	34
61	Thermal conductivity of giant mono- to few-layered CVD graphene supported on an organic substrate. Nanoscale, 2016, 8, 10298-10309.	2.8	34
62	Hot carrier transfer and phonon transport in suspended nm WS2 films. Acta Materialia, 2019, 175, 222-237.	3.8	34
63	Distinguishing Optical and Acoustic Phonon Temperatures and Their Energy Coupling Factor under Photon Excitation in nm 2D Materials. Advanced Science, 2020, 7, 2000097.	5.6	34
64	Characterization of thermal transport in micro/nanoscale wires by steady-state electro-Raman-thermal technique. Applied Physics A: Materials Science and Processing, 2009, 97, 19-23.	1.1	32
65	Thermal and Thermomechanical Phenomena in Picosecond Laser Copper Interaction. Journal of Heat Transfer, 2004, 126, 355-364.	1.2	31
66	Thermophysical properties of free-standing micrometer-thick Poly(3-hexylthiophene) films. Thin Solid Films, 2011, 519, 5700-5705.	0.8	31
67	Phonon energy inversion in graphene during transient thermal transport. Physics Letters, Section A: General, Atomic and Solid State Physics, 2013, 377, 721-726.	0.9	30
68	The structure of the "amorphous―matrix of keratins. Journal of Structural Biology, 2017, 198, 116-123.	1.3	30
69	19-Fold thermal conductivity increase of carbon nanotube bundles toward high-end thermal design applications. Carbon, 2018, 139, 445-458.	5.4	30
70	Anisotropic thermal transport in highly ordered TiO2 nanotube arrays. Journal of Applied Physics, 2009, 106, .	1.1	29
71	Thermal transport in single silkworm silks and the behavior under stretching. Soft Matter, 2012, 8, 9792.	1.2	28
72	Thermal transport across atomic-layer material interfaces. Nanotechnology Reviews, 2015, 4, .	2.6	28

#	Article	IF	CITATIONS
73	Energy coupling across low-dimensional contact interfaces at the atomic scale. International Journal of Heat and Mass Transfer, 2017, 110, 827-844.	2.5	28
74	Thermal transport and energy dissipation in two-dimensional Bi2O2Se. Applied Physics Letters, 2019, 115, .	1.5	28
75	Thermal characterization of submicron polyacrylonitrile fibers based on optical heating and electrical thermal sensing. Applied Physics Letters, 2006, 89, 152504.	1.5	27
76	Effect of zirconium(IV) propoxide concentration on the thermophysical properties of hybrid organic-inorganic films. Journal of Applied Physics, 2008, 104, .	1.1	27
77	Thermal transport in Si/Ge nanocomposites. Journal Physics D: Applied Physics, 2009, 42, 095416.	1.3	27
78	Solidification and epitaxial regrowth in surface nanostructuring with laser-assisted scanning tunneling microscope. Journal of Applied Physics, 2005, 98, 114304.	1.1	26
79	Co-existing heat currents in opposite directions in graphene nanoribbons. Physics Letters, Section A: General, Atomic and Solid State Physics, 2013, 377, 2970-2978.	0.9	26
80	Corrugated epitaxial graphene/SiC interfaces: photon excitation and probing. Nanoscale, 2014, 6, 8822.	2.8	25
81	Thermal conductivity of SiC microwires: Effect of temperature and structural domain size uncovered by 0 K limit phonon scattering. Ceramics International, 2018, 44, 11218-11224.	2.3	25
82	Thermal behavior of materials in laser-assisted extreme manufacturing: Raman-based novel characterization. International Journal of Extreme Manufacturing, 2020, 2, 032004.	6.3	25
83	Dynamics evolution of shock waves in laser–material interaction. Applied Physics A: Materials Science and Processing, 2009, 94, 675-690.	1.1	24
84	Thermally induced increase in energy transport capacity of silkworm silks. Biopolymers, 2014, 101, 1029-1037.	1.2	24
85	Very fast hot carrier diffusion in unconstrained MoS ₂ on a glass substrate: discovered by picosecond ET-Raman. RSC Advances, 2018, 8, 12767-12778.	1.7	24
86	Characterization of ultralow thermal conductivity in anisotropic pyrolytic carbon coating for thermal management applications. Carbon, 2018, 129, 476-485.	5.4	24
87	Characterization of anisotropic thermal conductivity of suspended nm-thick black phosphorus with frequency-resolved Raman spectroscopy. Journal of Applied Physics, 2018, 123, .	1.1	23
88	Viability of Neural Cells on 3D Printed Graphene Bioelectronics. Biosensors, 2019, 9, 112.	2.3	23
89	Near-field thermal transport in a nanotip under laser irradiation. Nanotechnology, 2011, 22, 075204.	1.3	21
90	Energy transport in crystalline DNA composites. AIP Advances, 2014, 4, .	0.6	21

6

#	Article	IF	CITATIONS
91	THERMAL CHARACTERIZATION OF MULTI-WALL CARBON NANOTUBE BUNDLES BASED ON PULSED LASER-ASSISTED THERMAL RELAXATION. Functional Materials Letters, 2008, 01, 71-76.	0.7	20
92	Microscale Spatially Resolved Thermal Response of Si Nanotip to Laser Irradiation. Journal of Physical Chemistry C, 2011, 115, 22207-22216.	1.5	20
93	3-dimensional anisotropic thermal transport in microscale poly(3-hexylthiophene) thin films. Polymer, 2013, 54, 1887-1895.	1.8	20
94	Strongly anisotropic thermal and electrical conductivities of a self-assembled silver nanowire network. RSC Advances, 2016, 6, 90674-90681.	1.7	20
95	Thermal reffusivity: uncovering phonon behavior, structural defects, and domain size. Frontiers in Energy, 2018, 12, 143-157.	1.2	20
96	PHOTOACOUSTIC TECHNIQUE FOR THERMAL CONDUCTIVITY AND THERMAL INTERFACE MEASUREMENTS. Annual Review of Heat Transfer, 2013, 16, 135-157.	0.3	20
97	Interfacial Thermal Conductance between Monolayer WSe ₂ and SiO ₂ under Consideration of Radiative Electron–Hole Recombination. ACS Applied Materials & Interfaces, 2020, 12, 51069-51081.	4.0	18
98	Thermophysical properties of hydrogenated vanadium-doped magnesium porous nanostructures. Nanotechnology, 2010, 21, 055707.	1.3	17
99	Nanoscale Probing of Thermal, Stress, and Optical Fields under Near-Field Laser Heating. PLoS ONE, 2013, 8, e58030.	1.1	17
100	Nanoparticles Formed in Picosecond Laser Argon Crystal Interaction. Journal of Heat Transfer, 2003, 125, 1147-1155.	1.2	16
101	EQUILIBRIUM MOLECULAR DYNAMICS STUDY OF PHONON THERMAL TRANSPORT IN NANOMATERIALS. Numerical Heat Transfer, Part B: Fundamentals, 2004, 46, 429-446.	0.6	16
102	Secondary shock wave in laser-material interaction. Journal of Applied Physics, 2008, 104, .	1.1	16
103	Sub-wavelength temperature probing in near-field laser heating by particles. Optics Express, 2012, 20, 14152.	1.7	16
104	Cross-plane thermal transport in micrometer-thick spider silk films. Polymer, 2014, 55, 1845-1853.	1.8	16
105	Interfacial Thermal Conductance between Mechanically Exfoliated Black Phosphorus and SiO <i>_x</i> : Effect of Thickness and Temperature. Advanced Materials Interfaces, 2017, 4, 1700233.	1.9	16
106	Sub-μm c-axis structural domain size of graphene paper uncovered by low-momentum phonon scattering. Carbon, 2018, 126, 532-543.	5.4	16
107	Polarized Raman of Nanoscale Two-Dimensional Materials: Combined Optical and Structural Effects. Journal of Physical Chemistry C, 2019, 123, 23236-23245.	1.5	16
108	Phase change and stress wave in picosecond laser–material interaction with shock wave formation. Applied Physics A: Materials Science and Processing, 2013, 112, 677-687.	1.1	15

#	Article	IF	CITATIONS
109	In situ investigation of annealing effect on thermophysical properties of single carbon nanocoil. International Journal of Heat and Mass Transfer, 2020, 151, 119416.	2.5	15
110	Coherency between thermal and electrical transport of partly reduced graphene paper. Carbon, 2021, 178, 92-102.	5.4	15
111	Hybrid atomistic-macroscale modeling of long-time phase change in nanosecond laser–material interaction. Applied Surface Science, 2008, 255, 3097-3103.	3.1	13
112	Thermal probing in single microparticle and microfiber induced near-field laser focusing. Optics Express, 2013, 21, 14303.	1.7	13
113	Efficient Solar-to-Thermal Energy Conversion and Storage with High-Thermal-Conductivity and Form-Stabilized Phase Change Composite Based on Wood-Derived Scaffolds. Energies, 2019, 12, 1283.	1.6	13
114	Nonlinear effects in transient electrothermal characterization of anatase TiO2 nanowires. Review of Scientific Instruments, 2012, 83, 044901.	0.6	12
115	Subâ€micron imaging of subâ€surface nanocrystalline structure in silicon. Journal of Raman Spectroscopy, 2013, 44, 1523-1528.	1.2	12
116	Thermal transport in graphene fiber fabricated by wet-spinning method. Materials Letters, 2016, 183, 147-150.	1.3	12
117	Identifying the Crystalline Orientation of Black Phosphorus by Using Optothermal Raman Spectroscopy. ChemPhysChem, 2017, 18, 2828-2834.	1.0	12
118	Significantly reduced <i>c</i> -axis thermal diffusivity of graphene-based papers. Nanotechnology, 2018, 29, 265702.	1.3	12
119	High thermal conductivity of free-standing skeleton in graphene foam. Applied Physics Letters, 2020, 117, .	1.5	12
120	Direct Characterization of Thermal Nonequilibrium between Optical and Acoustic Phonons in Graphene Paper under Photon Excitation. Advanced Science, 2021, 8, 2004712.	5.6	12
121	Nanodomain shock wave in near-field laser–material interaction. Physics Letters, Section A: General, Atomic and Solid State Physics, 2007, 369, 323-327.	0.9	11
122	Shock wave confinement-induced plume temperature increase in laser-induced breakdown spectroscopy. Physics Letters, Section A: General, Atomic and Solid State Physics, 2014, 378, 3319-3325.	0.9	11
123	Revealing the linear relationship between electrical, thermal, mechanical and structural properties of carbon nanocoils. Physical Chemistry Chemical Physics, 2018, 20, 13316-13321.	1.3	11
124	Rigorous prediction of Raman intensity from multi-layer films. Optics Express, 2020, 28, 35272.	1.7	11
125	Imaging Anisotropic Waveguide Exciton Polaritons in Tin Sulfide. Nano Letters, 2022, 22, 1497-1503.	4.5	11
126	Effects of laser fluence on near-field surface nanostructuring. Applied Surface Science, 2008, 254, 4201-4210.	3.1	10

#	Article	IF	CITATIONS
127	Interfacial thermal resistance between nm-thick MoS2 and quartz substrate: A critical revisit under phonon mode-wide thermal non-equilibrium. Nano Energy, 2021, 89, 106364.	8.2	10
128	Plume splitting in pico-second laser–material interaction under the influence of shock wave. Physics Letters, Section A: General, Atomic and Solid State Physics, 2009, 373, 3342-3349.	0.9	9
129	Across-plane thermal characterization of films based on amplitude-frequency profile in photothermal technique. AIP Advances, 2014, 4, 107122.	0.6	9
130	Structural evolution of nanoparticles under picosecond stress wave consolidation. Computational Materials Science, 2014, 95, 74-83.	1.4	9
131	Temperature dependent behavior of thermal conductivity of sub-5 nm Ir film: Defect-electron scattering quantified by residual thermal resistivity. Journal of Applied Physics, 2015, 117, .	1.1	9
132	Interface Energy Coupling between β-tungsten Nanofilm and Few-layered Graphene. Scientific Reports, 2017, 7, 12213.	1.6	9
133	Photocurrent in carbon nanotube bundle: Graded Seebeck coefficient phenomenon. Nano Energy, 2021, 86, 106054.	8.2	9
134	Thermophysical Properties of Lignocellulose: A Cell-Scale Study Down to 41K. PLoS ONE, 2014, 9, e114821.	1.1	9
135	Dynamic Structure and Mass Penetration of Shock Wave in Picosecond Laser-Material Interaction. Japanese Journal of Applied Physics, 2008, 47, 964-968.	0.8	8
136	Effect of molecular weight and density of ambient gas on shock wave in laser-induced surface nanostructuring. Journal Physics D: Applied Physics, 2009, 42, 015307.	1.3	8
137	Characterization of Thermal Transport in One-dimensional Solid Materials. Journal of Visualized Experiments, 2014, , e51144.	0.2	8
138	Energy and Charge Transport in 2D Atomic Layer Materials: Raman-Based Characterization. Nanomaterials, 2020, 10, 1807.	1.9	8
139	Significantly Reduced Anisotropic Phonon Thermal Transport in Graphene Oxide Films. Synthesis and Reactivity in Inorganic, Metal Organic, and Nano Metal Chemistry, 2013, 43, 1197-1205.	0.6	7
140	The in-plane structure domain size of nm-thick MoSe ₂ uncovered by low-momentum phonon scattering. Nanoscale, 2021, 13, 7723-7734.	2.8	7
141	Robust and high-sensitivity thermal probing at the nanoscale based on resonance Raman ratio (R3). International Journal of Extreme Manufacturing, 2022, 4, 035201.	6.3	7
142	Characterization of thermal transport across single-point contact between micro-wires. Applied Physics A: Materials Science and Processing, 2013, 110, 403-412.	1.1	6
143	Material behavior under extreme domain constraint in laser-assisted surface nanostructuring. Physics Letters, Section A: General, Atomic and Solid State Physics, 2016, 380, 753-763.	0.9	6
144	Thermal conductance between water and nm-thick WS ₂ : extremely localized probing using nanosecond energy transport state-resolved Raman. Nanoscale Advances, 2020, 2, 5821-5832.	2.2	6

#	Article	IF	CITATIONS
145	Effect of time and spatial domains on monolayer 2D material interface thermal conductance measurement using ns ET-Raman. International Journal of Heat and Mass Transfer, 2021, 179, 121644.	2.5	5
146	Dual-pace transient heat conduction in vertically aligned carbon nanotube arrays induced by structure separation. Nano Energy, 2021, 90, 106516.	8.2	5
147	Interface Thermal Resistance between Monolayer WSe ₂ and SiO ₂ : Raman Probing with Consideration of Optical–Acoustic Phonon Nonequilibrium. Advanced Materials Interfaces, 2022, 9, .	1.9	5
148	Effects of pressure and temperature on sp ³ fraction in diamondlike carbon materials. Journal of Materials Research, 2007, 22, 2770-2775.	1.2	4
149	Asymmetry of Raman scattering by structure variation in space. Optics Express, 2017, 25, 18378.	1.7	4
150	Farâ€Field Parallel Direct Writing of Subâ€Diffractionâ€Limit Metallic Nanowires by Spatially Modulated Femtosecond Vector Beam. Advanced Materials Technologies, 0, , 2200125.	3.0	4
151	Fabrication of Carbon Nanotube - Chromium Carbide Composite Through Laser Sintering. Lasers in Manufacturing and Materials Processing, 2016, 3, 1-8.	1.2	3
152	Effect of ethanol soaking on the structure and physical properties of carbon nanocoils. Diamond and Related Materials, 2019, 97, 107426.	1.8	3
153	Characterization of thermal transport in one-dimensional microstructures using Johnson noise electro-thermal technique. Applied Physics A: Materials Science and Processing, 2015, 119, 871-879.	1.1	1
154	Solid-to-super-critical phase change and resulting stress wave during internal laser ablation. Journal of Thermal Stresses, 2018, 41, 1364-1379.	1.1	1
155	Physics in Laser Near-Field Nanomanufacturing: Fundamental Understanding and Novel Probing. , 2015, , 1-20.		1
156	Thermomechanical effect induced by pulse laser heating. , 0, , .		0
157	Pulsed Laser Heating-induced Surface Rapid Cooling and Amorphization. Materials Research Society Symposia Proceedings, 2008, 1066, 1.	0.1	0
158	Far-field nanoscale thermal and structure imaging. , 2012, , .		0
159	Phonon transport manipulation and control in graphene for energy applications. , 2013, , .		0
160	Nanoparticle structure evolution under picosecond laser-induced stress wave compression. , 2014, , .		0
161	Physics in Laser Near-Field Nanomanufacturing: Fundamental Understanding and Novel Probing. , 2016, , 3195-3213.		0
162	Characterization of thermal conductivity, diffusivity, specific heat, and interface thermal resistance of carbon nanostructures. , 2020, , 57-89.		0